Available online at www.sciencedirect.com
ScienceDirect
Field Crops Research 102 (2007) 33–42
Field Crops Research
www.elsevier.com/locate/fcr

Assessing broadband vegetation indices and QuickBird data in estimating leaf area index of corn and potato canopies

Jindong Wu [a,*], Dong Wang [b], Marvin E. Bauer [a]

[a] Department of Forest Resources, University of Minnesota, 115 Green Hall, 1530 Cleveland Avenue North, St. Paul, MN 55108, USA
[b] Department of Soil, Water, and Climate, University of Minnesota, St. Paul, MN 55108, USA

Received 24 July 2006; received in revised form 10 January 2007; accepted 22 January 2007

Abstract

Leaf area index (LAI) is a key biophysical variable that can be used to derive agronomic information for field management and yield prediction. In the context of applying broadband and high spatial resolution satellite sensor data to agricultural applications at the field scale, an improved method was developed to evaluate commonly used broadband vegetation indices (VIs) for the estimation of LAI with VI–LAI relationships. The evaluation was based on direct measurement of corn and potato canopies and on QuickBird multispectral images acquired in three growing seasons. The selected VIs were correlated strongly with LAI but with different efficiencies for LAI estimation as a result of the differences in the stabilities, the sensitivities, and the dynamic ranges. Analysis of error propagation showed that LAI noise inherent in each VI–LAI function generally increased with increasing LAI and the efficiency of most VIs was low at high LAI levels. Among selected VIs, the modified soil-adjusted vegetation index (MSAVI) was the best LAI estimator with the largest dynamic range and the highest sensitivity and overall efficiency for both crops. QuickBird image-estimated LAI with MSAVI–LAI relationships agreed well with ground-measured LAI with the root-mean-square-error of 0.63 and 0.79 for corn and potato canopies, respectively. LAI estimated from the high spatial resolution pixel data exhibited spatial variability similar to the ground plot measurements. For field scale agricultural applications, MSAVI–LAI relationships are easy-to-apply and reasonably accurate for estimating LAI.

Keywords: Leaf area index; QuickBird; Remote sensing; Sensitivity; Stability; Vegetation index

1. Introduction

Remotely sensed measurements provide great potential for monitoring crop activities, although remote sensing cannot directly measure agronomic variables such as leaf area index (LAI) and crop biomass. To derive agronomic information for field management and yield prediction, mechanistic crop simulation models have been used to assimilate remote sensing data (Delécolle et al., 1992; Doraiswamy et al., 2004). Since LAI is a key state variable in crop models and drives photosynthesis, the assimilation is often achieved by directly updating LAI with remotely sensed LAI, and/or dynamically optimizing model parameters to obtain a simulation in agreement with remote-sensing estimated LAI (Moulin et al., 1998). In either case, the provision of reliable estimation of LAI using remotely sensed measurements is essential to the data assimilation and the analyses of temporal and spatial variability of crop conditions and productivity.

Numerous studies have attempted to estimate LAI with either physically based canopy radiative transfer models (RTMs) or empirical or semi-empirical relationships between spectral vegetation indices (VIs) and LAI. RTMs are based on the rigorous description of multi-scattering processes in canopies (Verhoef, 1984; Kuusk, 1994). The inversion of RTMs appears to be a promising method for the estimation of LAI from multispectral reflectances. A number of studies have inverted different RTMs to estimate the LAI of crop canopies (Goel and Thompson, 1984; Jacquemoud et al., 1995). Recently, Casa and Jones (2004) estimated LAI of potato canopies using a simplified ray tracing canopy model PROSAIL. The inversion was based on a look-up table approach with fixed leaf chlorophyll concentrations, leaf mesophyll structure, equivalent water thickness, dry matter content, and the hotspot parameter. Walthall et al. (2004) used a hybrid approach that combines an artificial neural network

* Corresponding author. Tel.: +1 612 624 3459; fax: +1 612 625 5212.
E-mail address: jindong@umn.edu (J. Wu).

0378-4290/$ – see front matter
doi:10.1016/j.fcr.2007.01.003

and a RTM to estimate corn and soybean LAI from Landsat ETM+ imagery. The hybrid approach avoids tedious iterations in the traditional model optimization and gives a relatively fast estimation of LAI once the training of neural network is completed.

Because of complex interactions between solar radiation and three-dimensional, heterogeneous, and anisotropic plant canopies, and the limited knowledge we have about radiative transfer processes, RTMs have not been fully developed and discrepant results have been found among models (Jacquemoud et al., 2000). The robustness of RTMs relies on the calibration of input parameters, e.g., leaf biochemical characteristics, soil optical properties, and canopy architecture, which are not routinely available for local crop species, soil conditions, and cultural practices. RTMs are also difficult to invert and computationally expensive for operational applications (Myneni et al., 1995). Therefore, RTMs are often restricted to specific ideal conditions of plants and environment (Gobron et al., 1997), and it is difficult to apply this method to agricultural practices.

The other and extensively studied way of estimating LAI from spectral reflectance data is to determine an empirical or semi-empirical VI–LAI relationship, and then invert the relationship using ground-based spectral measurements or satellite sensor data (Curran, 1983; Asrar et al., 1985; Wiegand et al., 1990; Turner et al., 1999; Vaesen et al., 2001). This method emphasizes practical considerations and is based on limited physical principles (Myneni et al., 1995), but it is simple and easy-to-apply. For the purposes of providing agricultural management information at the field scale, such relationships were still used in recent works (Walthall et al., 2004; Baez-Gonzalez et al., 2005).

Many VIs have been proposed to reduce non-vegetation effects and enhance the responsivity to the variations of canopy biophysical characteristics, e.g., LAI (Bannari et al., 1995). However, the stability and sensitivity of VIs are affected by several external perturbing factors, such as atmospheric conditions (Myneni and Asrar, 1994), soil optical properties (Huete, 1989), and illumination geometry (Shibayama et al., 1986). In addition, VIs are functions of multiple internal canopy factors, such as canopy morphology (e.g., leaf angle distribution) and leaf physiological properties (e.g., pigment content) (Haboudane et al., 2004).

From a practical point of view, all undesirable factors that may affect VI–LAI relationships have to be accounted for with simple and inexpensive procedures. To reduce atmospheric effects, VIs ideally should be computed with atmospherically corrected surface reflectances (Turner et al., 1999), which can be accurately retrieved from satellite sensor data with relatively simple algorithms (Wu et al., 2005). For agricultural field applications, remote sensing analyses are usually operated within a relatively small area such as a soil-mapping unit. At this scale, soil optical properties may be well represented by defining a soil line with respect to the specific soil type (Richardson and Wiegand, 1977; Baret et al., 1993). The effect of soil background can be reduced by integrating the parameters of the soil line (i.e., the slope and intercept in the red (R)–near infrared (NIR) spectral space) into soil-adjusted VIs.

Other factors that affect VI–LAI are mostly internal canopy variables, namely leaf angle distribution and pigment content. For monoculture crops planted in relatively homogeneous fields, leaf angle distribution may not change substantially during the growing season (Major et al., 1992). However, it is difficult to separate the variation of leaf pigment content in the construction of VI–LAI relationships (Haboudane et al., 2004) because leaf pigment content changes with LAI during crop growth and development. Vaesen et al. (2001) found in rice canopies that plant chlorophyll content did not add significant predictive power of VI–LAI relationships. In practice, field applications often require a general VI–LAI relationship that holds across the entire growing season with a wide variation of leaf pigment content.

VI–LAI relationships have been developed for a variety of crops: wheat (Asrar et al., 1985), rice (Vaesen et al., 2001), and corn (Wiegand et al., 1990; Baez-Gonzalez et al., 2005). Many studies have found significant variations of these relationships in accordance with the change of internal and external factors. However, none of these studies conducted sensitivity analyses to examine how noise levels inherent in VI–LAI relationships could have affected the accuracy of LAI estimation. On the basis of theoretically simulated spectra of crop canopies (soil and plant), only a few studies used leaf and canopy RTMs to evaluate potential errors in the estimation of LAI with VI–LAI relationships (Baret and Guyot, 1991; Bouman, 1992; Broge and Leblanc, 2000; Haboudane et al., 2004). However, as discussed earlier, the assumptions made in these models may have idealized canopy radiative conditions. The evaluations may also be biased by the choice of input parameters corresponding to specific conditions. In fact, these parameters often change with phenology (e.g., leaf pigment content) and environmental factors (e.g., soil moisture) in the field (Haboudane et al., 2004). Therefore, to account for diverse field conditions throughout the growing season, it would be necessary to use real field measurements to examine the efficiency of VIs.

The accuracy of LAI estimation should consider two aspects: absolute values and spatial variability. Most studies have only focused on the accuracy of absolute values of LAI. Little effort has been made to assess the capability of VI–LAI relationships in providing consistent spatial variability of crop conditions. The validation of the spatial variability of LAI has been challenged by difficulties in obtaining adequate ground measurements at the coarse spatial resolution of satellite sensor observations to represent spatial variances of the area under investigation (Tian et al., 2002). The successful launch of the QuickBird satellite (on 18 October 2001) has made the highest spatial resolution satellite data readily available to user communities and has provided new opportunities for remote sensing applications in agriculture (Wu et al., 2007). The high spatial resolution of QuickBird images makes it possible to match estimated pixel data with representative ground plot measurements, thus to evaluate the spatial variability of LAI.

While efforts have been made to design new hyperspectral indices to increase the sensitivity to LAI (Broge and Leblanc, 2000; Haboudane et al., 2004), it is important to evaluate the performance of existing broadband VIs in order to use most

available satellite data. Studies have shown that broadband VIs had similar efficiency to their narrowband counterparts (Elvidge and Chen, 1995) and were actually less affected by external factors when used as the estimators of LAI (Broge and Leblanc, 2000). This study was conducted within the framework of applying broadband visible and near infrared satellite sensor data to field scale agricultural practices. The objectives of the study were: (1) to develop appropriate methods to evaluate the efficiency of VI–LAI relationships for the estimation of LAI; (2) to analyze error propagation with actual field measurements made throughout the growing season; (3) to identify a broadband VI which has a relatively high efficiency for field scale applications; (4) to estimate high-resolution LAI from QuickBird data using the identified VI and to validate the absolute value and the spatial variability of estimated LAI.

2. Materials and methods

2.1. Field experiment

The experiment was carried out in two agricultural farms near Becker, MN. Over the growing seasons of 2002, 2003 and 2004, corn (*Zea mays* L.) was cultivated in a farmer-managed field (45°23′N, 93°50′W, 262.7 m), while potato (Russet Burbank) was cultivated in the Sand Plain Research Farm of the University of Minnesota (45°23′N, 93°53′W, 265.2 m). Soils in both fields were Hubbard loamy sand (Entic Hapludolls). Soil physical and chemical properties were assumed temporally constant and spatially uniform. Throughout each of the growing seasons, soil surface conditions mainly changed in wetness due to irrigation and rainfall events. The spectral reflectances of bare soil surface were measured using a Cropscan MSR-16R multiband radiometer (described below) to determine the soil line. Canopy reflectance and LAI were measured at different growth stages of the two crops and covered a wide range of LAI. Eleven campaigns in the corn field and 18 campaigns in the potato field were carried out from the beginning of June to the end of August. The datasets allow us to examine the responses of VIs to plant types and vegetation dynamics when soil optical properties are known and represented with a specific soil line.

2.2. Data collection

2.2.1. Canopy spectral reflectance measurement

Canopy spectral reflectances were measured with a 16-band multispectral radiometer (Cropscan MSR-16R, 0.46–1.72 μm). The radiometer simultaneously measures irradiance and radiance to provide canopy surface reflectances. The red (0.63–0.69 μm) and NIR (0.76–0.90 μm) spectrum, corresponding to the third and fourth band of QuickBird data, were simulated with appropriate Cropscan bands as weighted averages (Wu et al., 2005). The spectroradiometer was positioned looking vertically downward at 1 m above crop canopies with a 28° field of view (FOV). Measurements were taken around solar noon to minimize the effect of diurnal changes in solar zenith angle.

Ten intensive sampling areas (3 m × 3 m) were established along three transects across the corn field to capture the spatial variability based on the prior knowledge of soil and crop production zones. Multispectral reflectances were measured every 1 m along a row or a furrow and at 0.7 m interval across rows and furrows with the FOV centering over rows and furrows alternatively. In total, 27 measurements were taken per sampling area. Among them, 15 measurements were centered over rows and 12 measurements were centered over furrows. In the potato field, canopy reflectances were measured in 24 small nitrogen treatment plots (3.7 m × 6.1 m). Seven measurements were taken per plot, in which four measurements were centered over rows and three measurements were centered over furrows. Reflectance measurements were then averaged for each sampling area or plot to estimate a single reflectance value.

2.2.2. LAI measurement

LAI of crop canopies was measured with Li-Cor LAI-2000 plant canopy analyzer. The 270° view cap was used to remove the sun and the operator from the sensor's view. One above-canopy reading and three below-canopy readings were collected for each measurement. To increase the spatial coverage, below-canopy readings were made at even intervals along a diagonal transect between rows. Twelve measurements were taken per sampling area for corn and three measurements were taken per plot for potato. All measurements were averaged to obtain a single LAI value for each sampling area or plot.

2.2.3. Image acquisition and surface reflectance retrieval

Four QuickBird multispectral images covering both corn and potato fields were acquired under clear sky conditions on 22 June 2002, 20 June 2003, 18 July 2003, and 20 August 2004. The images have three visible bands (0.45–0.52 μm, 0.52–0.60 μm, and 0.63–0.69 μm) and one NIR band (0.76–0.90 μm). The spatial resolution of the 2002 and 2004 images is 2.8 m, while that of the 2003 images is 2.4 m. The images were geometrically rectified and radiometrically and atmospherically corrected to obtain surface reflectance (Wu et al., 2005). Each pixel corresponding to a sampling area or plot was geo-located with the Differential Global Positioning System (DGPS)–Ashtech Z-Surveyor measurements. The Ashtech Z-Surveyor is a real-time kinematic GPS unit with the horizontal root-mean-square-error (RMSE) of 1 cm.

2.3. Selected spectral vegetation indices

For the purpose of this study, five of the most commonly used and functionally different broadband VIs were selected (Bannari et al., 1995) (Table 1). These VIs were grouped into two categories based on the assumption of the orientation of isovegetation lines regarding to the soil line in the R–NIR spectral space: ratio-based indices and distance-based indices (Huete, 1989; Baret and Guyot, 1991). The most known and widely used ratio-based index is the normalized difference vegetation index (NDVI) (Rouse et al., 1974). NDVI is very sensitive to soil background at low LAI (Huete, 1989), and the sensitivity of NDVI to LAI weakens when LAI exceeds a

Table 1
Selected functionally different vegetation indices (VIs) and their references[a]

VI	Reference
NDVI = (NIR − R)/(NR + R)	Rouse et al. (1974)
SAVI = (1 + *L*)(NIR − R)/(NIR + R + *L*)	Huete (1988)
MSAVI = (NIR + 1) − (1/2)[(2NIR + 1)^2 − 8(NIR − R)]$^{1/2}$	Qi et al. (1994)
TSAVI = [*a*(NIR − *a*R − *b*)]/[*a*NIR +R − *ab* + *X*(1 + *a*^{2})]	Baret et al. (1989), Baret and Guyot (1991)
PVI = (NIR − *a*R − *b*)/(1 + *a*^{2})$^{1/2}$	Richardson and Wiegand (1977)

[a] NDVI, SAVI, MSAVI, TSAVI, and PVI are the normalized difference vegetation index, the soil-adjusted vegetation index, the modified soil-adjusted vegetation index, the transformed soil-adjusted vegetation index, and the perpendicular vegetation index, respectively. R and NIR are spectral radiance in the red and near infrared band, respectively. *L* and *X* are soil background adjustment factors. *a* and *b* are the slope and intercept of the soil line, respectively.

threshold value, which is typically around three (Carlson and Ripley, 1997).

Huete (1988) developed the soil-adjusted vegetation index (SAVI) by shifting the convergent point of isovegetation lines from the origin to a point in the quadrant of negative red and NIR values. Many studies have indicated that SAVI not only reduces the effect of soil variability for low LAI, but also increases the sensitivity to high LAI (Baret and Guyot, 1991; Elvidge and Chen, 1995). However, in order to determine the optimal value of the soil background adjustment factor *L*, prior knowledge about vegetation density or LAI is required, which creates a loop problem since LAI is the unknown target variable.

One approach for optimizing *L* was to replace the constant factor *L* with an empirical but dynamic function of *L* and thus formulate the modified soil-adjusted vegetation index $MSAVI_2$ (in this paper referred to as MSAVI) regardless of vegetation density (Qi et al., 1994). Another improvement with MSAVI is to allow for arbitrary slopes and intercepts of the soil line rather than to assume that the soil line has a slope of 1.0 and passes through the origin. MSAVI may be more applicable in practice because soil effects are implicitly adjusted according to different vegetation densities (i.e., soil parameters are not required for calculation). Studies using RTMs have found that MSAVI was the most sensitive VI to LAI (Broge and Leblanc, 2000).

Arbitrary slopes and intercepts of a soil line are also used in the transformed soil-adjusted vegetation index (TSAVI) (Baret et al., 1989; Baret and Guyot, 1991). As for SAVI, the convergent point of isovegetation lines has also been shifted from the origin into the third quadrant of the R–NIR spectral space. Baret and Guyot (1991) found that TSAVI was the best VI for low LAI compared with NDVI and SAVI, but gave the largest noise for high LAI.

The typical VI based on the second assumption is the perpendicular vegetation index (PVI) (Richardson and Wiegand, 1977), which accounts for the effect of soil background by computing an orthogonal greenness vector to a soil line with arbitrary slopes and intercepts. PVI reduced soil effects and held a near linear relationship with LAI for low LAI (Curran, 1983), but it introduced much noise at high LAI (Baret and Guyot, 1991).

The selected VIs, namely, NDVI, SAVI, MSAVI, TSAVI, and PVI, were computed with both ground-based canopy reflectance measurements and image-retrieved surface reflectances. The suggested optimal value of *L* (=0.5) and *X* (=0.08) were used in SAVI and TSAVI, respectively. The slope (1.450) and intercept (0.024) of the soil line were derived from ground measurements of bare soil surface. The red and NIR reflectances of bare soil varied from 0.03 to 0.15 and from 0.07 to 0.23, respectively.

2.4. Non-linear fitting of VI–LAI relationships

The general semi-empirical relationship between a VI and LAI can be expressed as an exponential function based on the modified Beer's law (Baret and Guyot, 1991):

$$\mathrm{VI} = \mathrm{VI}_\infty - (\mathrm{VI}_\infty - \mathrm{VI}_g)\exp(-K_{\mathrm{VI}}\mathrm{LAI}) \quad (1)$$

where VI_∞ is the asymptotically limiting value of a specific VI when LAI approaches a very large value; VI_g is the index value corresponding to bare soil conditions (LAI = 0). The dynamic range of the VI (i.e., $\mathrm{VI}_\infty - \mathrm{VI}_g$) is the difference between its maximum (VI_∞) and minimum value (VI_g). K_{VI} is the absorption-scattering coefficient that determines the sensitivity of the VI to a unit increase of LAI.

For a specific VI, these parameters depend on leaf angle distributions, soil optical properties, and solar zenith angles. In this study, reflectance measurements were taken for given crops cultivated on a given type of soil, and at the solar noon and the nadir view angle. Thus, the values of these parameters are expected to be less variable for each crop. Based on the large datasets measured in the three growing seasons, the Marquardt non-linear regression technique (Marquardt, 1963) was used to determine a set of best-fitted values with respect to each selected VI for both corn and potato canopies. The dynamic range of each VI, the standard deviation of each modeled parameter, and the RMSE and the adjusted coefficient of determination (r^2) were calculated to compare the fitted relationships.

2.5. Efficiency of VI–LAI relationships

The efficiency of a VI–LAI relationship in terms of retrieving LAI depends on three factors: the stability of the VI with other perturbing factors, the sensitivity of the VI to a unit change of LAI, and the dynamic range of the VI. Several methods have been developed to compare and evaluate the efficiency of VIs, such as the relative equivalent LAI noise ($\mathrm{REN}_{\mathrm{LAI}}$) (Baret and Guyot, 1991) and the signal-to-noise ratio (S/N) (LePrieur et al., 1994; Qi et al., 1994). But these methods do not account for all three factors. For instance, both $\mathrm{REN}_{\mathrm{LAI}}$ and S/N considered the stability, but $\mathrm{REN}_{\mathrm{LAI}}$ did not consider the dynamic range and S/N did not consider the sensitivity. The improved method (T_{VI}(LAI)) proposed by Gilabert et al. (1998) was modified and used in this study. T_{VI}(LAI) takes into

account all three factors and can be computed as a dynamic function of LAI:

$$T_{VI}(LAI) = \frac{\sigma_{LAI}(VI)}{\bar{\sigma}_{VI}} \times 100\% \quad (2)$$

where $\bar{\sigma}_{VI}$ is the average standard deviation of the whole range of VI values corresponding to all LAI levels, and $\sigma_{LAI}(VI)$ is the standard deviation or noise of LAI induced by the variation of VI values at a given time. $\bar{\sigma}_{VI}$ represents the dynamic range of the VI while $\sigma_{LAI}(VI)$ results from both the stability and the sensitivity of the VI–LAI relationship. Based on the theories of error propagation (Bevington, 1969), $\sigma_{LAI}(VI)$ or the error propagated to the final result of LAI because of the uncertainties in VI can be expressed as,

$$\sigma_{LAI}(VI) = \sigma_{VI}\left(\frac{d\,LAI}{d\,VI}\right) \quad (3)$$

where σ_{VI} is the standard deviation or stability of the VI corresponding to a given value of LAI, and d LAI/d VI is the reversed local slope of VI–LAI relationships and represents the sensitivity of VI to LAI change. Therefore, by combing Eqs. (2) and (3), the method we used to evaluate the efficiency of VI–LAI relationships was expressed as,

$$T_{VI}(LAI) = \left(\frac{\sigma_{VI}}{\bar{\sigma}_{VI}}\right)\left(\frac{d\,VI}{d\,LAI}\right)^{-1} \times 100\% \quad (4)$$

where d VI/d LAI is the first-order derivative deduced from Eq. (1). T_{VI} values decrease as the efficiency of VI–LAI relationships increases since a VI with high efficiency should be sensitive to vegetation density (with high d VI/d LAI), but insensitive to other perturbing factors (with low σ_{VI}), and have a large dynamic range of variations (with high $\bar{\sigma}_{VI}$). Based on ground-based measurements and the VI–LAI relationships fitted with Eq. (1), the dynamic change of T_{VI} values as a function of LAI were computed for all selected VIs with respect to each crop.

2.6. Estimation and validation of LAI from QuickBird imagery data

The VI with the lowest T_{VI} values was regarded as the most efficient VI (VI^e) for the estimation of LAI. To test the accuracy of LAI estimated with VI^e, we inverted the VI^e–LAI relationship to estimate LAI from QuickBird imagery data (Eq. (5)):

$$LAI = -\left(\frac{1}{K_{VI^e}}\right)\ln\left[\frac{VI^e_\infty - VI^e}{VI^e_\infty - VI^e_g}\right] \quad (5)$$

where VI^e values were computed with the atmospherically corrected QuickBird surface reflectances; VI^e_∞, VI^e_g, and K_{VI^e} are parameters of the VI^e–LAI function determined with Eq. (1). The other selected VIs were discarded because of the low efficiency.

The algorithm was applied to each ground sampling area for both crops. Estimates of LAI were plotted against the corresponding ground measurements of each sampling area. Compared with satellite sensors with coarse spatial resolutions in heterogeneous landscapes, it is reasonably accurate to scale up ground point measurements by averaging to the spatial resolution of QuickBird images in relatively homogeneous agricultural fields (Curran and Williamson, 1986). We thus made direct comparison between the QuickBird image-estimated pixel values and the average values of ground measurements.

To validate the spatial variability of LAI, the spatial cumulative distribution function (SCDF) was computed to represent the spatial statistical characteristics of image-estimated and ground-measured LAI. SCDF or F(LAI) was defined as the probability that LAI takes a value less than or equal to a given value in a spatial domain (Evans et al., 2000). For each crop, F(LAI) of image-estimated and ground-measured LAI were compared to determine the differences in representing spatial heterogeneity at the field scale.

3. Results and discussion

3.1. VI–LAI relationships

All VIs were strongly correlated with LAI (Table 2). The correlations were significant even though the measurements were taken throughout the entire growing season under varied field conditions, which indicated that the change of the VIs was mainly governed by LAI. Among them, SAVI, MSAVI, TSAVI, and PVI showed the highest correlation with LAI ($r^2 \sim 0.8$ for corn and $r^2 \sim 0.9$ for potato) while NDVI showed the lowest correlation for both crops ($r^2 \sim 0.7$). It was evident that the parameters in the VI–LAI relationships varied with indices and there were no generic values for all VIs. Additionally, the fitted parameters varied considerably. Although this did not affect the strength of the correlations, it suggested the effect of unaccounted perturbing factors by the specific index.

Since both crops were planted on the same type of soil, VI_g values (for bare soil) were identical for corn and potato. Generally, VI_g for the ratio-based VIs were larger than zero, particularly VI_g for NDVI was as large as 0.27 because of not adjusting soil effects. VI_∞ values (for dense vegetation) for NDVI, TSAVI, and PVI changed with crops due to different leaf and canopy properties. However, it appeared that VI_∞ values for SAVI and MSAVI were relatively consistent for different crops. Actually, we found that all parameters for MSAVI (VI_g, VI_∞, and K_{VI}) were close between corn and potato, which may be explained by the fact that there is no empirical adjustment for vegetation density in the MSAVI equation (Table 1). As a result of differences in VI_g and VI_∞ among VIs, the dynamic ranges of VIs are quite different (Fig. 1). For both crops, MSAVI had the largest dynamic range of 0.83 while PVI had the smallest (0.43 for corn and 0.51 for potato) (Table 2). For the ratio-based VIs, NDVI had the smallest dynamic range (0.68 for corn and 0.63 for potato).

All VIs increased almost linearly with increasing LAI at low LAI levels until a threshold value (LAI_t) was reached, and then entered an asymptotic regime in which VIs increased very slowly with increasing LAI (Fig. 1). However, LAI_t varied with

Table 2
Best-fitted values of the parameters in vegetation index (VI)–leaf area index (LAI) relationships and statistics[a]

VI	NDVI	SAVI	TSAVI	MSAVI	PVI
Corn					
VI_g	0.27 (0.11[b])	0.11 (0.08)	0.00 (0.10)	0.11 (0.09)	0.00 (0.03)
VI_∞	0.95 (0.09)	0.86 (0.06)	0.76 (0.08)	0.94 (0.07)	0.43 (0.03)
$VI_\infty - VI_g$	0.68	0.75	0.76	0.83	0.43
K_{VI}	0.68 (0.14)	0.52 (0.09)	0.62 (0.11)	0.50 (0.10)	0.33 (0.08)
LAI_t	3.8	4.8	4.5	5.0	6.7
r^2	0.71	0.80	0.78	0.78	0.80
RMSE	0.07	0.07	0.07	0.08	0.04
Potato					
VI_g	0.27 (0.09)	0.11 (0.06)	0.00 (0.07)	0.11 (0.06)	0.00 (0.03)
VI_∞	0.90 (0.09)	0.86 (0.05)	0.73 (0.07)	0.94 (0.05)	0.51 (0.04)
$VI_\infty - VI_g$	0.63	0.75	0.73	0.83	0.51
K_{VI}	1.03 (0.13)	0.54 (0.07)	0.77 (0.09)	0.50 (0.07)	0.24 (0.06)
LAI_t	2.9	4.7	3.9	5.0	7.3
r^2	0.72	0.88	0.84	0.89	0.90
RMSE	0.04	0.04	0.04	0.05	0.03

[a] NDVI, SAVI, TSAVI, MSAVI, and PVI are the normalized difference vegetation index, the soil-adjusted vegetation index, the transformed soil-adjusted vegetation index, the modified soil-adjusted vegetation index, and the perpendicular vegetation index, respectively. VI_g is the index value corresponding to bare soil conditions; VI_∞ is the asymptotic value of a VI; $VI_\infty - VI_g$ is the dynamic range of a VI; K_{VI} is the sensitivity coefficient of a VI–LAI relationship. LAI_t is the threshold value of LAI when a VI reaches VI_∞. RMSE is the root-mean-square-error of a VI. r^2 is the adjusted coefficient of determination.
[b] Values in parentheses are the standard deviations of corresponding parameters.

the type of VI used. NDVI and TSAVI reached LAI_t of 2.9–3.8 and 3.9–4.5, respectively, while SAVI and MSAVI continued to increase up to LAI_t around 5. LAI_t for PVI varied with crops but was generally higher than 6. The sensitivity coefficient, K_{VI}, changed correspondingly with the largest value for NDVI and TSAVI. That is, NDVI and TSAVI increased rapidly with increasing LAI and reached LAI_t earlier than SAVI and MSAVI. PVI was characterized by the slowest variation within the smallest dynamic range.

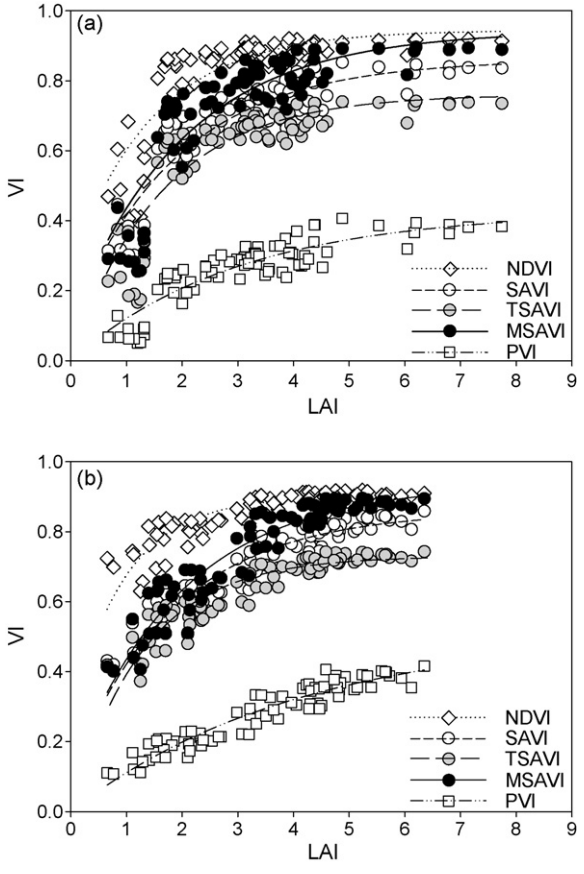

Fig. 1. Responses of vegetation indices (VIs) to leaf area index (LAI) for (a) corn and (b) potato canopies. Curves are the non-linear fitting of the responses.

3.2. Efficiency of VI–LAI relationships for LAI estimation

The sensitivity of the selected VIs consistently decreased as the amount of vegetation increased (Fig. 2). All VIs became much less sensitive to high LAI for dense canopies. It was found that d VI/d LAI of MSAVI was generally larger than that of other indices throughout the whole range of LAI variation.

T_{VI} values varied with the level of LAI (Fig. 3). All VIs except NDVI for potato had similar low T_{VI} values at low LAI ($1 < LAI < 2$). Thus, no VI appeared to be superior to another in reducing the effect of soil background. For potato canopies with $1 < LAI < 2$, because of the substantial expose of bare soil, NDVI apparently caused more error in the estimation of LAI than other VIs. Due to the shortage of measurements in the early part of growing seasons, the behavior of VIs cannot be concluded for $LAI < 1$ when the fraction of vegetation cover was very low.

T_{VI} values for dense canopies with high LAI were generally larger than those for sparse canopies (Fig. 3), indicating that the efficiency of VIs was reduced at high LAI levels. However, for both crops, T_{VI} values of MSAVI were consistently smaller than other VIs. In particular when $LAI \geq 4$, the differences of T_{VI} between MSAVI and the indices that had the 'worst' performance (PVI for corn and NDVI for potato) were evident. For dense potato canopies, T_{VI} of MSAVI even tended to decrease (Fig. 3). The results showed that MSAVI considerably reduced the noise in the estimation of LAI compared with other indices and it was the best LAI estimator. Similar results were

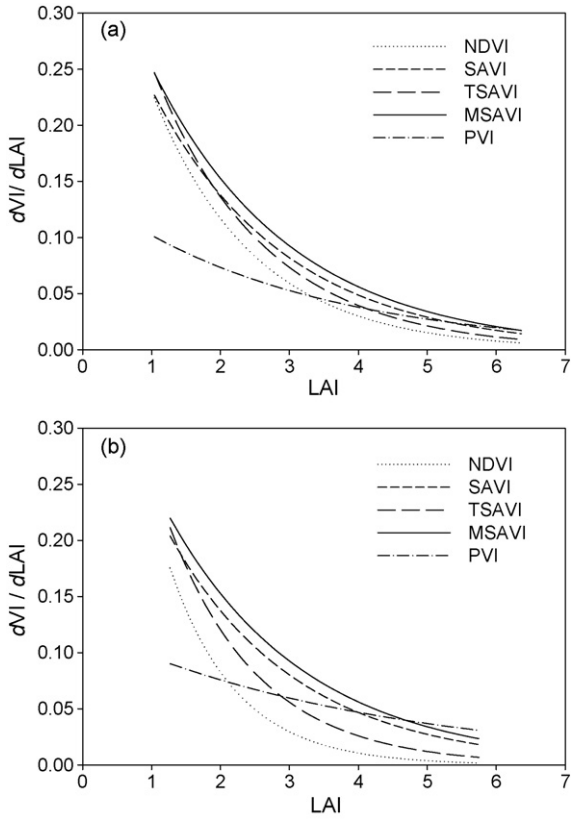

Fig. 2. Sensitivity (d VI/d LAI) of vegetation indices (VIs) to the change of leaf area index (LAI) at different LAI levels for (a) corn and (b) potato canopies.

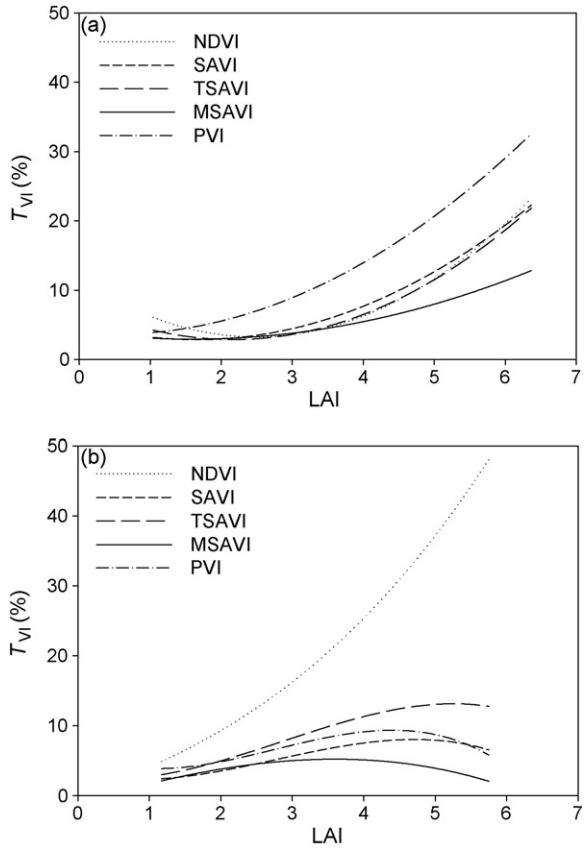

Fig. 3. Error propagation in the estimation of leaf area index (LAI) at different LAI levels for (a) corn and (b) potato canopies. T_{VI} (%) is the efficiency index of relative LAI noise inherent in the vegetation index (VI)–LAI functions.

found in earlier studies using RTMs (Broge and Leblanc, 2000). As discussed, the parameters in the MSAVI–LAI relationships were relatively consistent for both crops, suggesting it might be advantageous for other crops as suggested for soybean and wheat based on simulation studies (Haboudane et al., 2004).

The efficiency of NDVI, SAVI, TSAVI, and PVI varied with crops. For corn, the performance of NDVI was similar to SAVI and TSAVI and much better than PVI; while for potato, NDVI produced the largest error and SAVI and PVI proved to be slightly better than TSAVI. It should be noted that PVI had relatively high correlation with LAI ($r^2 = 0.8$ for corn and $r^2 = 0.9$ for potato), but the overall efficiency of PVI was actually not satisfactory because of the small dynamic range (Table 2) and the low sensitivity (Fig. 2). For corn canopies when LAI < 3 and for potato canopies when LAI < 2, the sensitivity of PVI was particularly low compared with other indices.

3.3. Comparison of estimated and measured LAI

Based on the evaluation of the efficiency of VI–LAI relationships, the MSAVI–LAI functions were inverted (Eq. (5)) to estimate LAI from four atmospherically corrected QuickBird images. The results indicated that the LAI estimates were in good agreement with the corresponding ground measurements (Fig. 4). The slope was 1.02 for corn and 0.97 for potato, and the corresponding RMSE was 0.63 and 0.79, respectively (Table 3). Because positives and negatives were canceled out in

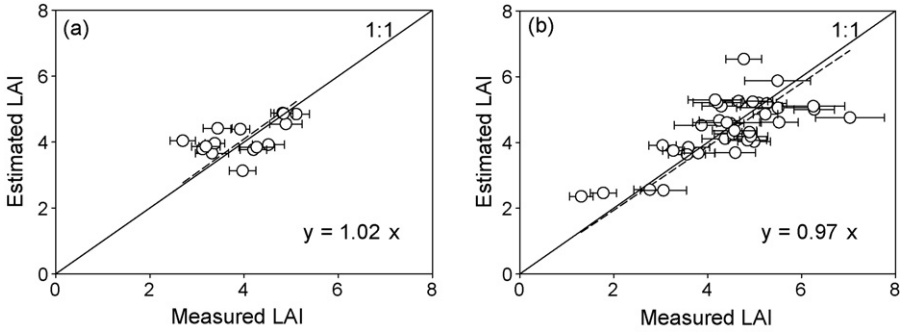

Fig. 4. QuickBird images-estimated leaf area index (LAI) and corresponding ground-based measurements for (a) corn and (b) potato canopies.

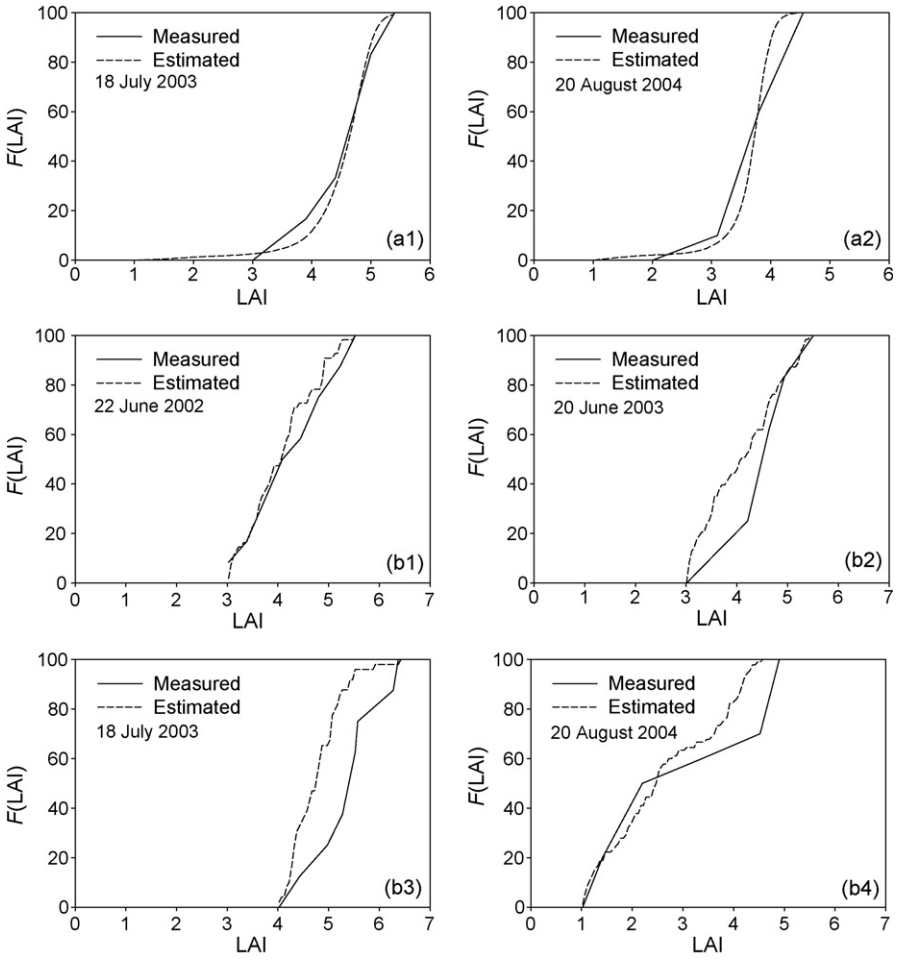

Fig. 5. Spatial cumulative distribution functions (F(LAI)) of leaf area index (LAI) estimated from the QuickBird images and concurrently measured in the fields for (a1–a2) corn and (b1–b4) potato canopies.

the comparison, the mean-absolute-difference (MAD) between estimated and measured LAI was even lower (0.18 for corn and −0.03 for potato). The overall accuracy was satisfactory considering that the average error of LAI measurements was on the order of 0.3 for corn and 0.5 for potato. Particularly for potato at high LAI levels (LAI > 5) when canopy leaves were densely clumped, the measurement error could be as large as 0.7–0.8. This might have led to the increased dispersion of the data points presented in the scatter plot (Fig. 4b). It appeared that LAI for corn canopies tended to be overestimated when LAI < 4 and underestimated when LAI > 4, but the uncertainty remains to be tested with more low and high LAI values since most LAI present in the scenes were in the mid-range.

Table 3
Statistical comparison of the image-estimated and the ground-measured leaf area index (LAI)[a]

	a	t^*	RMSE	MAD
Corn	1.02	25.44	0.63	0.18
Potato	0.97	33.39	0.79	−0.03

[a] a is the slope of the linear regression between the estimated and the measured LAI by forcing the intercept to be zero. t^* indicates a values are significant at $\alpha = 0.001$. RMSE and MAD are the corresponding root-mean-square-error and the mean-absolute-difference.

3.4. LAI spatial cumulative probability distributions

The F(LAI) generated with the QuickBird imagery data were generally close to the corresponding F(LAI) derived with the ground measurements (Fig. 5). Two pairs of comparison were made for corn canopies and four pairs of comparison were made for potato canopies on different dates. The comparisons indicated that LAI estimated from the high spatial resolution pixel data was able to demonstrate similar spatial variability of the plot measurements on the ground. For corn canopies, the SCDF of the image-estimated LAI only slightly deviated from the ground measurements (Fig. 5a). For potato canopies, both SCDFs agreed well at low LAI levels (LAI < 3) (Fig. 5b4). At high LAI levels (LAI > 3), the agreement varied with images but the image-estimated LAI tended to have higher F(LAI) compared with the ground measurements (Fig. 5b).

4. Conclusions

An improved method was developed to evaluate the efficiency of commonly used broadband VIs in estimating LAI. The method took into account all three factors that affect the efficiency of VIs, i.e., stabilities, sensitivities, and dynamic ranges. Based on field measurements made in three growing

seasons, we analyzed LAI noise inherent in each VI–LAI function and examined the capacity of QuickBird data for monitoring absolute LAI values and spatial variabilities.

LAI dominated the variation of canopy spectral reflectances and all VIs were strongly correlated with LAI, but with different efficiencies for LAI estimation. LAI noise generally increased with increasing LAI. For dense canopies, the efficiency of most VIs was highly reduced. The best behavior was given by MSAVI, which had the largest dynamic range and the highest sensitivity and overall efficiency for both crops. The differences in the performance between MSAVI and other indices were particularly evident at high LAI levels.

QuickBird image-estimated LAI using the inverted MSAVI–LAI relationship agreed well with ground measurements in both absolute values and spatial variability. The evaluation and validation were based on corn and potato, and the parameters of MSAVI–LAI were relatively consistent for different crops. Thus, the results should have implications for other crops. For the purpose of agricultural applications at the field scale, the semi-empirical MSAVI–LAI relationships are reasonably efficient for estimating LAI with satisfactory absolute values and spatial variability. It was difficult to schedule ground measurements concurrently with commercial satellite overpasses. More coordinated ground measurements and QuickBird images, particularly in the early growing season, are needed for the future validation.

Acknowledgements

The authors wish to acknowledge the grant from USDA/NASA 2001-52103-11321 for providing QuickBird images and the grant from the University of Minnesota Graduate School Grant-In-Aid for supporting ground measurement. We greatly appreciate the constructive suggestions of two anonymous reviewers. We also thank Dr. Carl Rosen and Mr. Frank Kasowski for providing field sites, Dr. Yi Zhang, Dr. Kurt Spokas, and Mr. Matt McNearney for general assistance with ground measurements.

References

Asrar, G., Kanemasu, E.T., Yoshida, M., 1985. Estimates of leaf area index from spectral reflectance of wheat under different cultural practices and solar angle. Remote Sens. Environ. 17, 1–11.

Baez-Gonzalez, A.D., Kiniry, J.R., Maas, S.J., Tiscareno, M.L., Macias, J.C., Mendoza, J.L., Richardson, C.W., Salinas, J.G., Manjarrez, J.R., 2005. Large-area maize yield forecasting using leaf area index based yield model. Agron. J. 97, 418–425.

Bannari, A., Morin, D., Bonn, F., Huete, A.R., 1995. A review of vegetation indices. Remote Sens. Rev. 13, 95–120.

Baret, F., Guyot, G., 1991. Potentials and limits of vegetation indices for LAI and APAR assessment. Remote Sens. Environ. 35, 161–173.

Baret, F., Guyot, G., Major, D.J., 1989. TSAVI: a vegetation index which minimizes soil brightness effects on LAI and APAR estimation. In: Proceedings of the 12th Canadian Symposium on Remote Sensing IGARRS'90, Vancouver, Canada, pp. 1355–1358.

Baret, F., Jacquemoud, S., Hanocq, J.F., 1993. The soil line concept in remote sensing. Remote Sens. Rev. 7, 65–82.

Bevington, P.R., 1969. Data Reduction and Error Analysis for the Physical Sciences. McGraw-Hill Book Company, New York.

Bouman, B.A.M., 1992. Accuracy of estimating the leaf area index from vegetation indices derived from crop reflectance characteristics, a simulation study. Int. J. Remote Sens. 16, 3069–3084.

Broge, N.H., Leblanc, E., 2000. Comparing prediction power and stability of broadband and hyperspectral vegetation indices for estimation of green leaf area index and canopy chlorophyll density. Remote Sens. Environ. 76, 156–172.

Carlson, T.N., Ripley, D.A., 1997. On the relation between NDVI, fractional vegetation cover, and leaf area index. Remote Sens. Environ. 62, 241–252.

Casa, R., Jones, H.G., 2004. Retrieval of crop canopy properties: a comparison between model inversion from hyperspectral data and image classification. Int. J. Remote Sens. 25, 1119–1130.

Curran, P.J., 1983. Multispectral remote sensing for the estimation of green leaf area index. Philos. T. Roy. Soc. A 309, 257–270.

Curran, P.J., Williamson, H.D., 1986. Sample size for ground and remotely sensed data. Remote Sens. Environ. 20, 31–41.

Delécolle, R., Maas, S.J., Guérif, M., Baret, F., 1992. Remote sensing and crop production models: present trends. ISPRS J. Photogramm. 47, 145–161.

Doraiswamy, P.C., Hatfield, J.L., Jackson, T.J., Akhmedova, B., Prueger, J., Stern, A., 2004. Crop condition and yield simulations using Landsat and MODIS. Remote Sens. Environ. 92, 548–559.

Elvidge, C.D., Chen, Z., 1995. Comparison of broadband and narrow-band red and near infrared vegetation indices. Remote Sens. Environ. 54, 38–48.

Evans, M., Hastings, N., Peacock, B., 2000. Statistical Distributions, 3rd ed. John Wiley, New York.

Gilabert, M.A., González-Piqueras, J., García-Haro, J., Meliá, J., 1998. Designing a generalized soil-adjusted vegetation index (GESAVI). In: Engman, E.T. (Ed.), Remote Sensing for Agriculture, Ecosystems and Hydrology, Proceedings of the SPIE, vol. 3499. pp. 396–404.

Gobron, N., Pinty, B., Verstraete, M.M., 1997. Theoretical limits to the estimation of the leaf area index on the basis of visible and near-infrared remote sensing data. IEEE T. Geosci. Remote Sens. 35, 1438–1445.

Goel, N.S., Thompson, R.L., 1984. Inversion of vegetation canopy reflectance models for estimating agronomic variables. V. Estimation of leaf area index and average leaf angle using measured canopy reflectances. Remote Sens. Environ. 16, 69–85.

Haboudane, D., Miller, J.R., Pattey, E., Zarco-Tejada, P.J., Strachan, I.B., 2004. Hyperspectral vegetation indices and novel algorithms for predicting green LAI of crop canopies: modeling and validation in the context of precision agriculture. Remote Sens. Environ. 90, 337–352.

Huete, A.R., 1988. A soil-adjusted vegetation index (SAVI). Remote Sens. Environ. 25, 295–309.

Huete, A.R., 1989. Soil influences in remotely sensed vegetation-canopy spectra. In: Asrar, G. (Ed.), Theory and Application of Optical Remote Sensing. Wiley, New York, pp. 107–141.

Jacquemoud, S., Baret, F., Andrieu, B., Danson, F.M., Jaggard, K.W., 1995. Extraction of vegetation biophysical parameters by inversion of the PROSPECT+SAIL models on sugar beet canopy reflectance data: application to TM and AVIRIS sensors. Remote Sens. Environ. 52, 163–172.

Jacquemoud, S., Bacour, C., Poilve, H., Frangi, J.-P., 2000. Comparison of four radiative transfer models to simulate plant canopies reflectance: direct and inverse mode. Remote Sens. Environ. 74, 417–481.

Kuusk, A., 1994. A multispectral canopy reflectance model. Remote Sens. Environ. 50, 75–82.

LePrieur, D., Verstraete, M.M., Pinty, B., 1994. Evaluation of the performance of various vegetation indices to retrieve cover from AVHRR data. Remote Sens. Rev. 10, 265–284.

Major, D.J., Schaalje, G.B., Wiegand, C., Blad, B.L., 1992. Accuracy and sensitivity analysis of SAIL model-predicted reflectance of maize. Remote Sens. Environ. 41, 61–70.

Marquardt, D.W., 1963. An algorithm for least squares estimation of nonlinear parameters. J. Soc. Ind. Appl. Math. 11, 431–441.

Moulin, S., Bondeau, A., Delecolle, R., 1998. Combining agricultural crop models and satellite observations: from field to regional scales. Int. J. Remote Sens. 19, 1021–1036.

Myneni, R.B., Asrar, G., 1994. Atmospheric effects and spectral vegetation indices. Remote Sens. Environ. 47, 390–402.

Myneni, R.B., Maggion, S., Iaquinta, J., Privette, J.L., Gobron, N., Pinty, B., Verstraete, M.M., Kimes, D.S., Williams, D.L., 1995. Optical remote sensing of vegetation: modeling, caveats and algorithms. Remote Sens. Environ. 51, 169–188.

Qi, J., Chehbouni, A., Huete, A.R., Kerr, Y.H., Sorooshian, S., 1994. A modified soil adjusted vegetation index. Remote Sens. Environ. 48, 119–126.

Richardson, A.J., Wiegand, C.L., 1977. Distinguishing vegetation from soil background information. Photogramm. Eng. Remote Sens. 43, 1541–1552.

Rouse, J.W., Haas Jr., R.H., Schell, J.A., Deering, D.W., 1974. Monitoring Vegetation Systems in the Great Plains with ERTS. In: NASA SP-351, 3rd ERTS-1 Symposium, Washington, DC, pp. 309–317.

Shibayama, M., Wiegand, C.L., Richardson, A.J., 1986. Diurnal patterns of bidirectional vegetation indices for wheat canopies. Int. J. Remote Sens. 7, 233–246.

Tian, Y., Woodcock, C.E., Wang, Y., Privette, J.L., Shabanov, N.V., Zhou, L., Zhang, Y., Buermann, W., Dong, J., Veikkanen, B., Hame, T., Andersen, K., Ozdogan, M., Knyazikhin, Y., Myneni, R.B., 2002. Multiscale analysis and validation of the MODIS LAI product. I. Uncertainty assessment. Remote Sens. Environ. 83, 414–430.

Turner, D.P., Cohen, W.B., Kennedy, R.E., Fassnacht, K.S., Briggs, J.M., 1999. Relationships between leaf area index and Landsat TM spectral vegetation indices across three temperate zone sites. Remote Sens. Environ. 70, 52–68.

Vaesen, K., Gilliams, S., Nackaerts, K., Coppin, P., 2001. Ground-measured spectral signatures as indicators of ground cover and leaf area index: the case of paddy rice. Field Crop. Res. 69, 13–25.

Verhoef, W., 1984. Light scattering by leaf layers with application to canopy reflectance modeling: the SAIL model. Remote Sens. Environ. 16, 125–141.

Walthall, C., Dulaney, W., Anderson, M., Norman, J., Fang, H., Liang, S., 2004. A comparison of empirical and neural network approaches for estimating corn and soybean leaf area index from Landsat ETM+ imagery. Remote Sens. Environ. 92, 465–474.

Wiegand, C.L., Gerbermann, A.H., Gallo, K.P., Blad, B.L., Dusek, D., 1990. Multisite analyses of spectral-biophysical data for corn. Remote Sens. Environ. 33, 1–16.

Wu, J., Wang, D., Bauer, M.E., 2005. Image-based atmospheric correction of QuickBird imagery of Minnesota cropland. Remote Sens. Environ. 99, 315–325.

Wu, J., Wang, D., Rosen, C.J., Bauer, M.E., 2007. Comparison of petiole nitrate concentrations, SPAD chlorophyll readings, and QuickBird satellite imagery in detecting nitrogen status of potato canopies. Field Crop. Res. 101, 96–103.